AE-374
UDC 539.173.8:546.791
539.122.16

AE-374

Gamma Radiation from Fission Fragments

J. Higbie

AKTIEBOLAGET ATOMENERGI
STUDSVIK, NYKÖPING, SWEDEN 1969

GAMMA RADIATION FROM FISSION FRAGMENTS

J. Higbie

ABSTRACT

The gamma radiation from the fragments of the thermal neutron fission of ^{235}U has been investigated, and the preliminary data are presented here with suggestions for further lines of research and some possible interpretations of the data. The data have direct bearing on the fission process and the mode of fragment de-exitation. The parameters measured are the radiation decay curve for the time interval $(1 - 7) \times 10^{-10}$ sec after fission, the photon yield, the total gamma-ray energy yield, and the average photon energy. The last three quantities are measured as a function of the fragment mass.

Printed and distributed in October 1969.

CONTENTS

INTRODUCTION

This investigation proceeds along lines very similar to the one carried out by Johansson (1) on the fragments of spontaneously fissioning ^{252}Cf. Since the fragments from thermal neutron fission of ^{235}U, which are examined here, are very similar to the fragments from ^{252}Cf, the reader is referred to Johansson's work for a more thorough discussion of these findings and their physical significance. Johansson's work will be referred to frequently here, and it should be understood in the following that reference 1 is indicated.

EXPERIMENTAL PROCEDURE

A. Apparatus

The apparatus used in this investigation is described in some detail in reference 2. Schematic diagrams of the experimental arrangement and the electronics are given in figures 1 and 2. The neutron beam indicated in figure 1 is taken from the core of the thermal neutron reactor R-2. The beam is filtered by a cooled quartz single crystal to reduce the fast neutron and gamma-ray content.

The fissile deposit is supported in the neutron beam on a thin nickel foil which allows the passage of fission fragments with only a small loss of fragment energy.

The fragment energies are measured by two opposed, heavy ion detectors which also serve to supply the fast timing signals required for the coincidence measurements. The whole assembly is contained in an evacuated fission chamber.

The fragment mass, used as a parameter in these measurements, is determined from the fragment energies alone. The determination is performed "on line" by the circuit indicated in figure 2 as the "Logarithimc Amplifier". This circuit furnishes a pulse which is proportional in height to a function of the fragment mass.

The life time of the emitted gamma-radiation is examined by the lead collimator indicated in figure 1. The principle employed is the time-of-flight of the fission fragments. Since these fragments have a velocity of the order of 1 cm/nsec, a considerably better time definition can be achieved in this manner than by electronic methods.

The gamma-radiation detector is a 5" x 4" NaI (Tl) scintillator placed 40 cm from the fission foil in order to allow a time-of-flight separation between the fission photons and neutrons. A typical time-of-flight spectrum is shown in figure 3. The photon peak at C has a FWHM of 5.5 nsec.

B. Resolution

When reference is made to the fragment mass, it should be understood that the initial mass is indicated, since it is on this basis that the initial fragment energies are determined. Moreover, the initial fragment mass is the physically significant parameter. For a mass determination using the fragment energies alone, it is a certain ratio of the final fragment energies which is involved. This calculation gives rise to an apparent or observed mass. Due to the various energy losses to which the fragments are subject before and during detection, it will be seen that a given apparent mass contains a distribution of initial masses. The most important energy dispersions arise from neutron evaporation and losses due to the fissile layer thickness. The resulting mass dispersion is treated in some detail in reference 2, and it is from the analysis found there that the mass assignments to the data points are made in this present work. The rms dispersion of initial fragment masses for each of the data points is indicated by the horizontal bars in the figures.

C. Measurements

The gamma-ray energy spectra were measured as a function of the apparent fragment mass using the electronics indicated in figure 2. The data were accumulated in a 64 x 64 channel matrix of the two parameter analyser. All events were gated by the time-to-pulse-height converter to assure that they belonged to the photon peak of the time-of-flight spectrum (the peak at C in figure 3). In this way, all neutron events were excluded, and only the random background needed to be subtracted from the measured data. The collimator setting used for these measurements corresponded to the time interval of (0.2 - 1.8) x 10^{-10} sec after fission.

It was, unfortunately, not possible to continuously monitor the background radiation for these measurements, and therefore the background contribution is somewhat uncertain. In order to continuously monitor the background, additional electronics would have been required. Based on background determinations taken at intervals during the experimental run, the background was estimated to be about 30% of the total, and it is for this value that the data were evaluated. The values of 36% and 10% are felt to represent the extreme possible limits, and the resulting change in the positions of the data points using these values for the background contribution is indicated in the figures.

For these measurements, the stability of the apparent mass spectrum is of great importance, and therefore the system was checked frequently for spectrum drift. The importance is due to the fact that all the derived results are normalized to the apparent mass yield, so that the calculated data points are "per-fragment" results and thus are quite sensitive to a relative shift along the fragment mass axis. This is a particularly vulnerable point for fission fragment studies, as the mass yield exhibits such large variations, and it is suggested, therefore, that efforts should be made in the future to eliminate this potential difficulty by extension of the electronics to incorporate an additional parameter, so that the "ungated" mass yield can be taken up in parallel with the "gated" data.

The decay curve for the total radiation was measured by means of the adjustable collimator of figure 1. The measurements were made for the light and heavy fragment groups respectively, but otherwise the decay was not investigated as a function of the fragment mass. The total radiation was measured from about 5 keV upwards.

The data was accumulated in a one parameter analyser, and it was the time-of-flight spectrum (figure 3) which was measured as a function of the collimator setting. An external gate was employed which examined the fragment energy spectrum from one of the fragment detectors and thereby determined to which of the two groups the detected fragment belonged. A substantially better time definition can be achieved in this manner than by considering all fragments in

the same measurement. According to the data of Milton and Fraser (3), the velocity dispersion (and therefore the time dispersion) for fragments belonging to one of the two mass yield groups is of the order of 5%. However, when all fragments are considered in the same measurement, the velocity dispersion rises to about 20%.

For all measured points on the decay curve except the last point, i.e., the furthest from the fission foil, the collimator opening was 1 mm. For this last, most distant position, the collimator opening was 2 mm. The corresponding time duration is then $\sim$ 135 and $\sim$ 270 psec respectively. The time duration is, of course, dependent upon whether light or heavy fragments are being observed. The effective width of the collimator is somewhat larger than 1 mm (or 2 mm) due to the experimental geometry and edge effects of the collimator. The design of the collimator deserves special attention, as it represents the limiting factor for good time resolution work. The collimator used in this work was rather crude and has since been improved upon. However, for the time regions measured here, the collimator was satisfactory. Improvements are necessary when one wishes to examine the fast component of the prompt radiation (see reference 1).

RESULTS

A. Treatment of data

The treatment of the radiation decay data was straight forward. The background for each of the experimental runs was obtained by closing the collimator completely and measuring the resultant time-of-flight spectrum until a statistically significant number of counts were accumulated. The counts in the photon peak are normalized to the number of fragments detected, and then the normalized background is subtracted. The width of the effective time interval is used to determine the counting rate per fragment. The results of these measurements are shown in figure 4. The dashed line in figure 4 corresponds to the fast component of the prompt radiation as measured by Johansson.

Corrections for the resolution width of the collimator were not attempted, since in the region of interest, i.e., the slow component of the prompt radiation, the correction is insignificant. In the region

of the fast component, the correction depends heavily upon the assumed mode of decay. The functional form of the decay curve is thereby changed, but, as discussed by Johansson, the calculated half-life of the radiation is about the same.

The gamma-ray energy spectra were grouped into mass intervals of approximately the mass resolution width, since a finer subdivision of the data cannot yield further information. The energy spectra were then "unfolded" using the detector responce matrix measured by Bergquist (4). This response matrix also takes into account the efficiency of the scintillator for the various gamma-ray energies. The desired spectrum parameters were then measured from the resulting photon spectra. The rms uncertainties in the measured values are indicated as the vertical bars in figures 5 - 7 and take into account the uncertainty introduced by the "unfolding" procedure as well as the counting and background statistics.

Since the event counting rate was so low, the resulting photon energy spectra reveal only the broadest type of structure. However, several general parameters may be measured from these spectra and these are given in figures 5 - 7.

B. Discussion

Since the fragment mass yield is rather strongly peaked at A = 96, 140, one would normally expect the decay curves of figure 4 to correspond to the radiation emitted from these two, rather narrow, fragment mass intervals. This may indeed by the case; however, we cannot assume with certainty that it is so until an investigation of the decay as a function of the fragment mass is carried out. Very little is known about the origin of this slow component, since most measurements to date have been concerned with the characteristics of the total radiation

from all fragments. The fact that this more detailed information is not available seriously inhibits any detailed interpretation of the gamma-ray energy spectra measured in this interval.

Johansson (1) has shown that the total gamma-ray energy yield for the fast component of the prompt radiation has the "saw-tooth" form of the neutron yield curve. However, in his treatment of the delayed component ($\sim$ 50 nsec), given in reference 6, the radiation yield is very different from the "saw-tooth" form. The results of his analysis indicate the existance of stably deformed nuclei in the light mass peak and confirms their existance for mass numbers greater than $\sim$ 148. Therefore, in this slow component of the prompt radiation, one may expect to see a deviation in the radiation yield curve from the "saw-tooth" form of the fast component. A slight indication that this is so is given by the fact that the total photon yield for the heavy fragment group is somewhat less than the yield for the light fragment group, as indicated by figure 4. The half-life of this slow component is measured to be $\sim 1.5 \times 10^{-10}$ sec.

Since the gamma-ray energy spectra were measured for the time interval $(0.2 - 1.8) \times 10^{-10}$ sec after fission, we can see from figure 4 that these measurements contain approximately equal amounts of the fast and slow components of the prompt radiation. An analysis of this data will have to take into account the properties of both components.

Johansson (1, 5) has interpreted the gamma-radiation to consist mainly of vibrational transitions. The energy spectra measured here also exhibit the characteristics of vibrational transitions in that a pronounced "bump" is seen at about 700 - 800 keV. This bump is felt to arise from a vibrational cascade in which all members of the transition would have equal energies in the harmonic potential approximation. Johansson (1) also saw this bump at 700 keV, but the high energy tail of his spectra was less pronounced than for these measurements. The slow component is therefore thought to consist mainly of the relatively fast (10^{-11} sec) vibrational cascade, with the important difference that the first member of the cascade is rather slow, and the measured half-life of the slow component thus corresponds to this first

transition. The first member of the cascade would therefore be a rather low energy transition which is consistent with the findings of Dési et al. (6) who reported a half-life between 10^{-9} and 10^{-10} sec for the radiation in the range 25 keV to 100 keV.

Examination of figures 5 and 6 reveals a tendency for deviation from the "saw-tooth" form of the fragment excitation curve in the mass region A = 85 to 90. It is well known that in this region, beginning from A = 90 and proceeding downwards toward the magic fragment A = 82, the fragments get progressively more "magic". That is, the deformation parameter makes a sharp increase in this region corresponding to an increased "stiffness" or resistance to deformation. Johansson (5) found that the magic nucleus ^{132}Sn exhibited delayed radiation with a half-life of the order of 50 nsec. This was interpreted as being due to a compression of the upper levels of the vibrational cascade. If we assume that the departure seen in figures 5 and 6 is due to the slow component, then it is also reasonable to assume that the delay in this case arises from a similar compression of the upper levels of the vibrational cascade. However, this interpretation must be considered to be rather preliminary.

In the mass interval approaching the magic fragment A = 128 from above, the yield curves show no tendency to increase. We may therefore assume that the relative gamma-ray energy yield for the fragment, A = 128, is quite low both for the fast and the slow components of the prompt radiation. Furthermore, the relative yield of the delayed radiation was reported by Johansson (5) to be rather low. Thus, if this fragment exhibits delayed radiation, it is limited to a region around 10 nsec or regions greater than 100 nsec. It is also noteworhty to observe that the neutron yield for this fragment, as reported by Terrell (7), is zero. (Terrell's results for the neutron yield are plotted as the curve in figure 5).

The systematics of the energy of the first 2^+ level in even-even nuclei show a pronounced upswing in the region of magic nuclei. Such an upswing in the average photon energy for the region approaching A = 128 is shown in figure 7. The same upswing in the average photon energy for masses approaching the magic fragment A = 82 is not observed. However, it is interesting to note that the average center-of-mass neutron kinetic energy, measured for Cf fragments by Bowman et al. (8), shows a very similar mass dependence to that of the average photon energy seen in figure 7.

The radiation from these otherwise quite similar magic fragments, A = 82, 128, is therefore seen to exhibit pronounced differences. These differences can yield information concerning the conditions at scission and the level structure for these two fragments. The conditions at scission are not quite the same in the two cases, in that the sister fragment to A = 82 is known to have a stable ground state deformation, whereas the sister fragment to A = 128 probably does not. Otherwise, it is generally assumed that these two magic fragments receive approximately the same amount of initial excitation energy. If this is indeed true, one should expect to find a delayed component of the gamma-radiation for the fragment A = 128.

The relatively high yield and increase in the average photon energy in the mass region A > 140 gives further evidence for the high initial spin of the fragments, as discussed by Johansson (1). The fragments in this region are deformed, and if one assumes a statistical distribution of quasi-particle levels, the variation seen in figure 7 should not occur. That such a variation is seen gives evidence not only to the interpretation of high initial fragment spin ($\sim 10\,\hbar$) but also indicates that the spin increases with increasing fragment excitation. (See reference 1 for a more complete discussion.)

In the mass region A = 105 to 110, the fragments become progressively softer to deformation. This can be seen from the deformation parameters as given, for example, by Terrell (9). Indeed, Johansson (5) has reported a region of stable deformation for fragments with A = 110. The relatively high gamma-ray energy yield and the tendency for an increase in the average photon energy at A = 105 seen in figures 6 and 7 can therefore be given the same interpretation as above, i.e., it is due to easily deformed fragments with high initial spin.

It is interesting to note, in passing, that the total gamma-radiation decay measured during a certain time interval after fission has a measured half-life comparable with the interval of measurement. This effect is mainly experimental in that components with appreciably faster or slower decay rates will have a correspondingly low intensity in the region considered. However, the existance of these decay rates is noteworthy and reflects the properties of high lying states in fission fragments, i.e., neutron-rich nuclei; but before we can hope to obtain further knowledge from this information, a systematic study of this decay rate as a function of the fragment mass must be performed.

CONCLUSIONS

The results presented here indicate the potential usefulness of such a study in determining the properties of nuclei far off the line of nuclear stability. In particular, we have stressed the ability of this method to determine the conditions at scission. Especially interesting is the behaviour seen in the vicinity of the magic fragments A = 82 and 128. It is hoped that these preliminary results will stimulate a further investigation in this region.

The gamma-radiation seen in this work is consistent with the interpretation of vibrational, quadropole transitions as postulated by Johansson (1). It may be assumed then that vibrational cascades play a predominant role in fission fragment gamma-ray de-excitation.

ACKNOWLEDGEMENTS

The author wishes to express his gratitude to Prof. S.A.E. Johansson for guidance in the theoretical interpretation of the results and many useful suggestions during the construction of the experimental apparatus.

The author is also indebted to Tekn. lic. H. Albinsson for his assistance and cooperation during the experimental phase.

Many thanks are extended to Docent Nils Starfelt who initially sponsored this project and Docent T. Wiedling who has been very helpful in the preparation of the manuscript.

FIGURE CAPTIONS

Figure 1 Schematic diagram of the experimental arrangement.

Figure 2 Block diagram of the electronic circuits.

Figure 3 A representative radiation time-of-flight spectrum.

Figure 4 Radiation decay curve for the slow component of the prompt radiation. The fast component is indicated by the broken line.

Figure 5 Gamma-ray photon yield. The solid curve is the neutron yield as reported by Terrell (7).

Figure 6 Total gamma-ray energy yield

Figure 7 Average gamma-ray photon energy.

REFERENCES

1. JOHANSSON, S.A.E.,
Gamma de-excitation of fission fragments. (I) Prompt radiation.
Nucl. Phys. 60 (1964) p. 378.

2. HIGBIE, J.,
Gamma radiation from fission fragments experimental apparatus - mass spectrum resolution. 1969.
(AE-367.)

3. MILTON, J.C.D., and FRASER, J.S.,
Time-of-flight fission studies on U^{233}, U^{235}, and Pu^{239}.
Can. J. Phys. 40 (1962) p. 1626.

4. BERGQUIST, I.,
Private communication.

5. JOHANSSON, S.A.E.,
Gamma de-excitation of fission fragments. (II) Delayed radiation.
Nucl. Phys. 64 (1965) p. 147.

6. DESI, S., LAJTAI, A., and NAGY, L.,
The time distribution of the gamma radiation emitted in the fission of U^{235}.
Acta. Phys. Acad. Sci. Hung., 15 (1962) p. 185.

7. TERRELL, J.,
Neutron yields from individual fission fragments.
Phys. Rev. 127 (1962) p. 880.

8. BOWMAN, H.R., et al.,
Further studies of the prompt neutrons from the spontaneous fission of Cf^{252}.
Phys. Rev. 129 (1963) p. 2133.

9. TERRELL, J.,
Prompt neutrons from fission.
Physics and chemistry of fission.
Proc. of a symp. Salzburg, 22-26 March 1965.
(IAEA) Vienna, 1965. Vol. 2, p. 3.

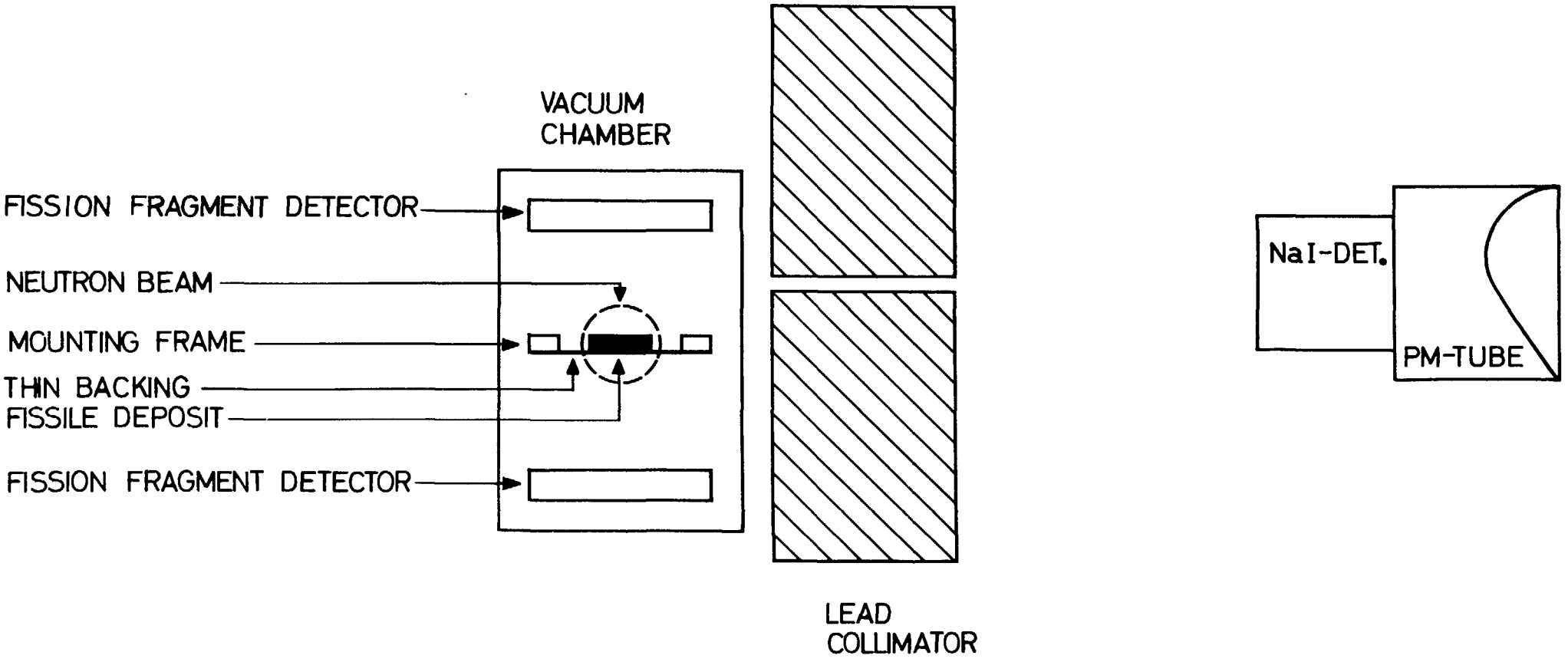

Fig. 1. Schematic diagram of the experimental arrangement

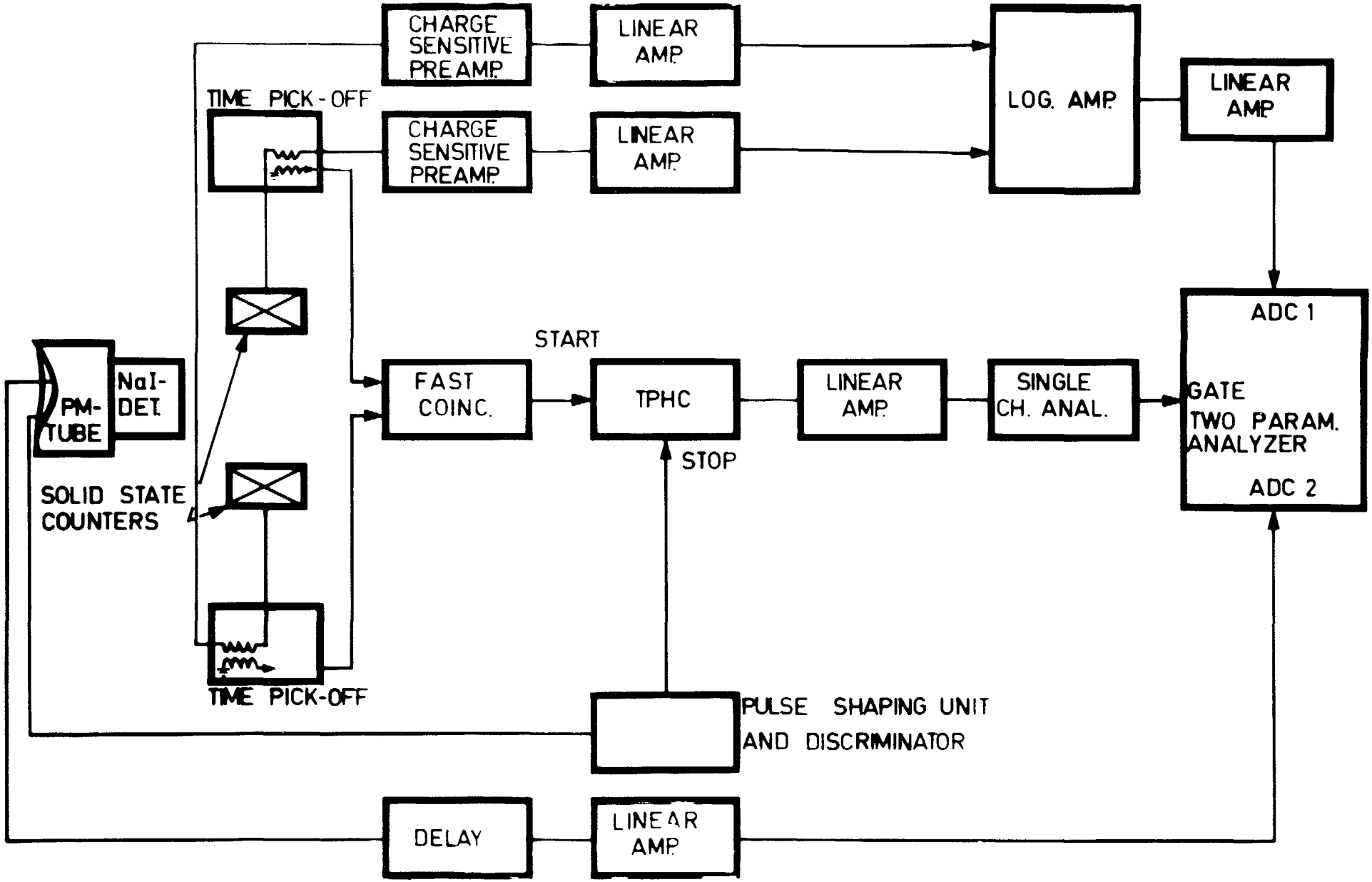

Fig. 2. Block diagram of the electronics

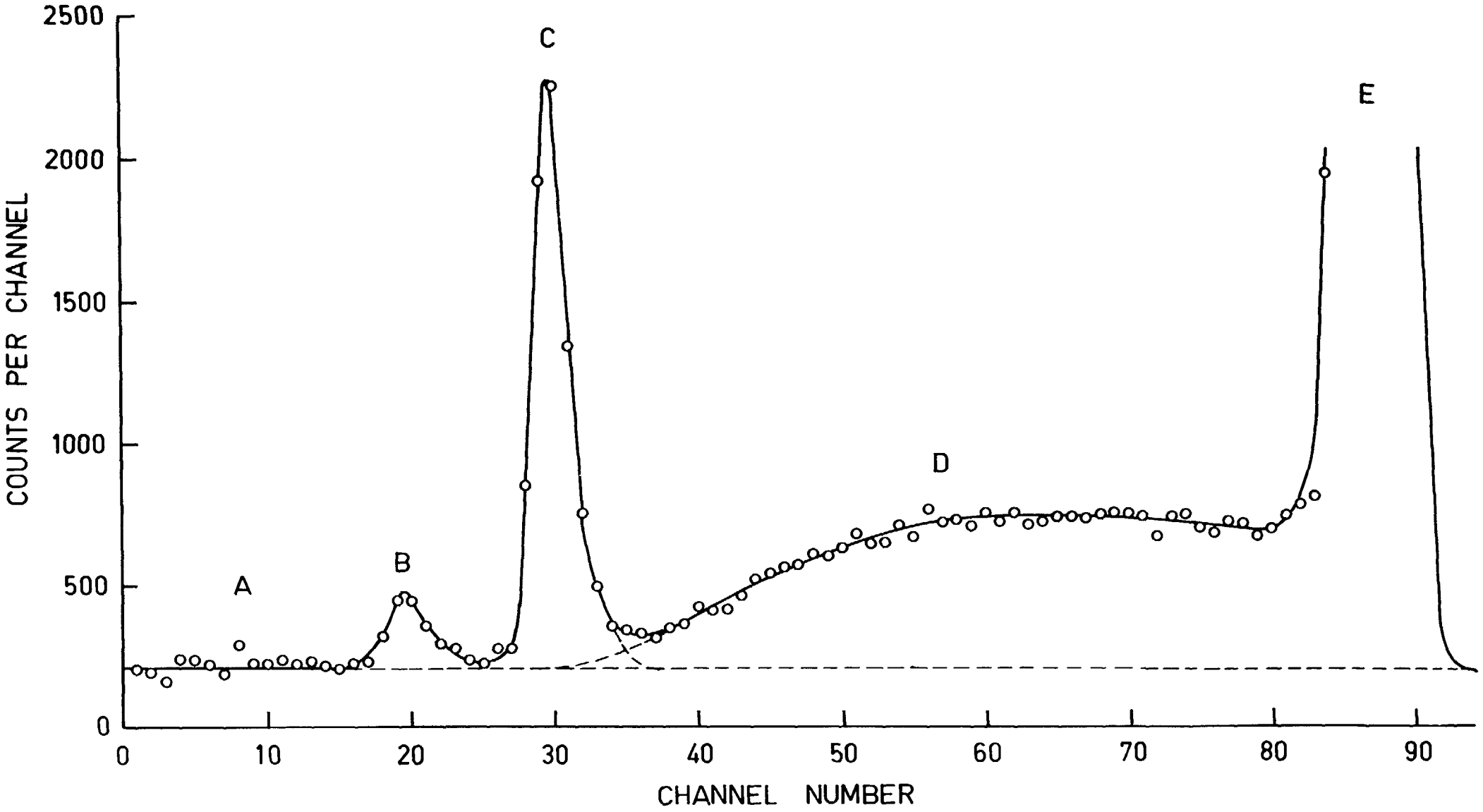

Fig. 3. A representative time-of-flight spectrum. The photon peak at C has a FWHM of 5.5 nsec. The region at D is the fission neutron contribution. A indicates the random background and E is the full sweep peak corresponding to the absence of a stop pulse. The peak at B is due to pulse pile-up

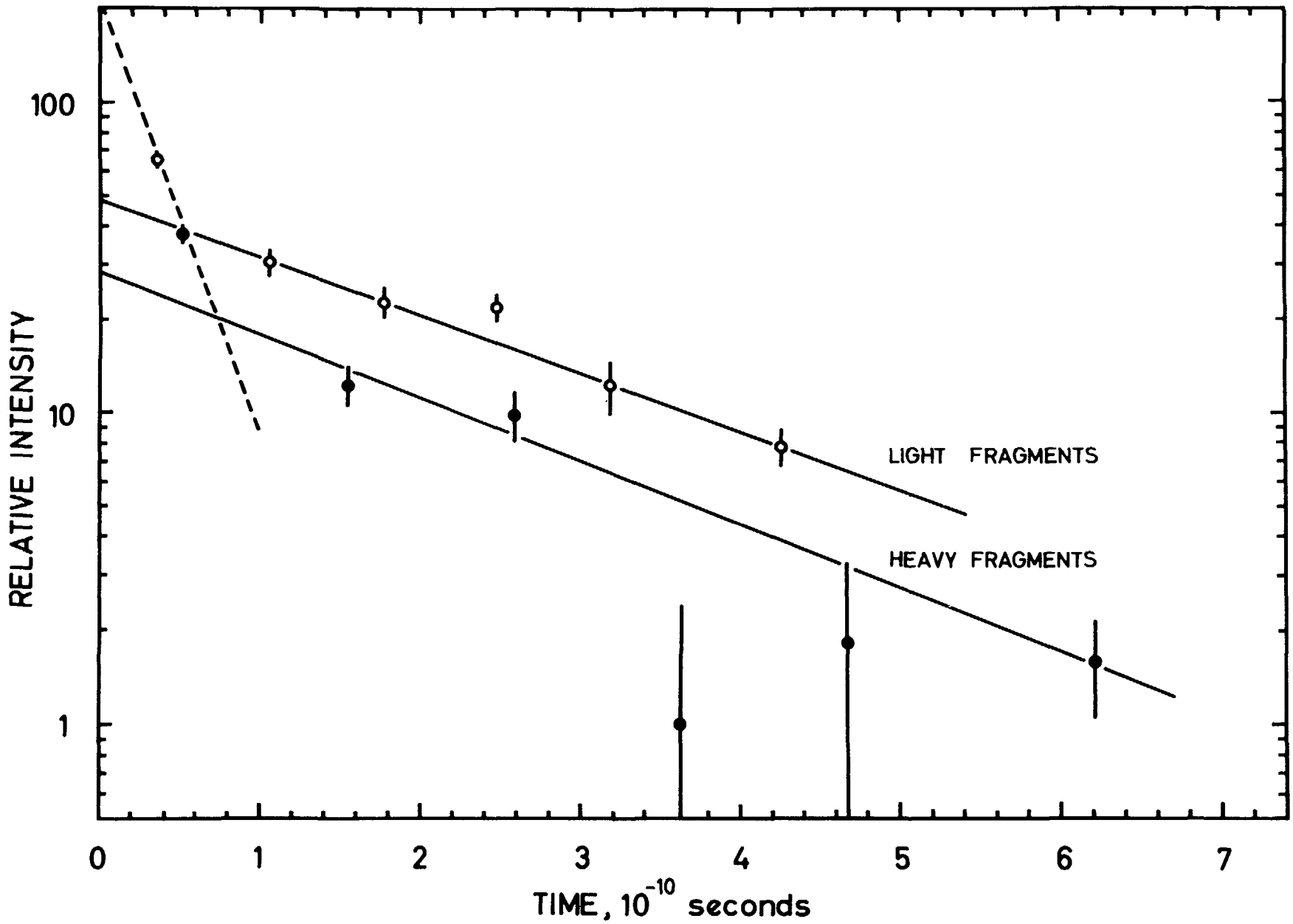

Fig. 4. The measured radiation decay curve. The half-lives indicated by the solid lines are 1.5×10^{-10} seconds. The fast component of the prompt radiation is indicated by the broken line

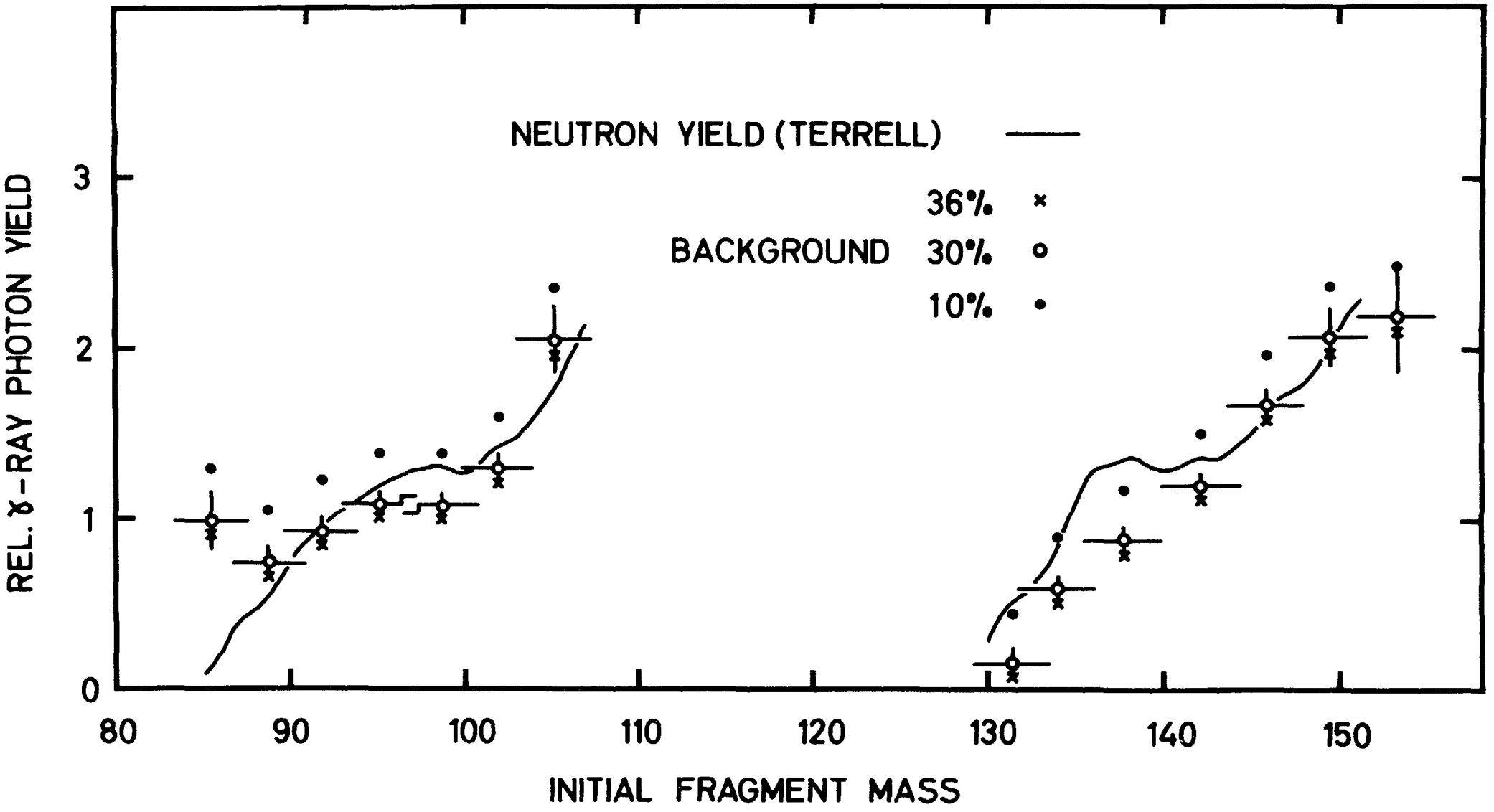

Fig. 5. The gamma-ray photon yield. The solid curve is the neutron yield as reported by Terrell (7)

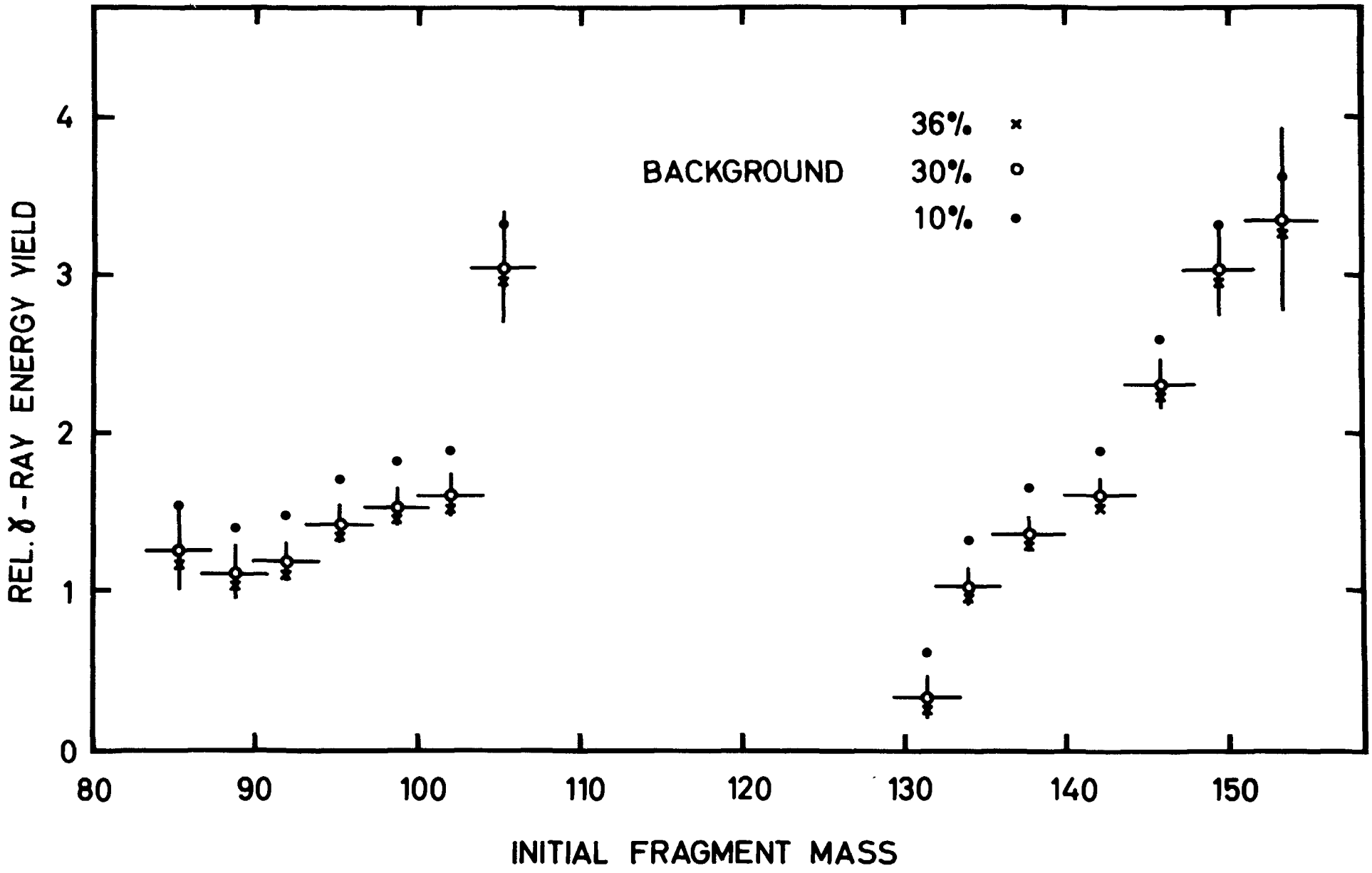

Fig. 6. The yield of the gamma-radiation energy

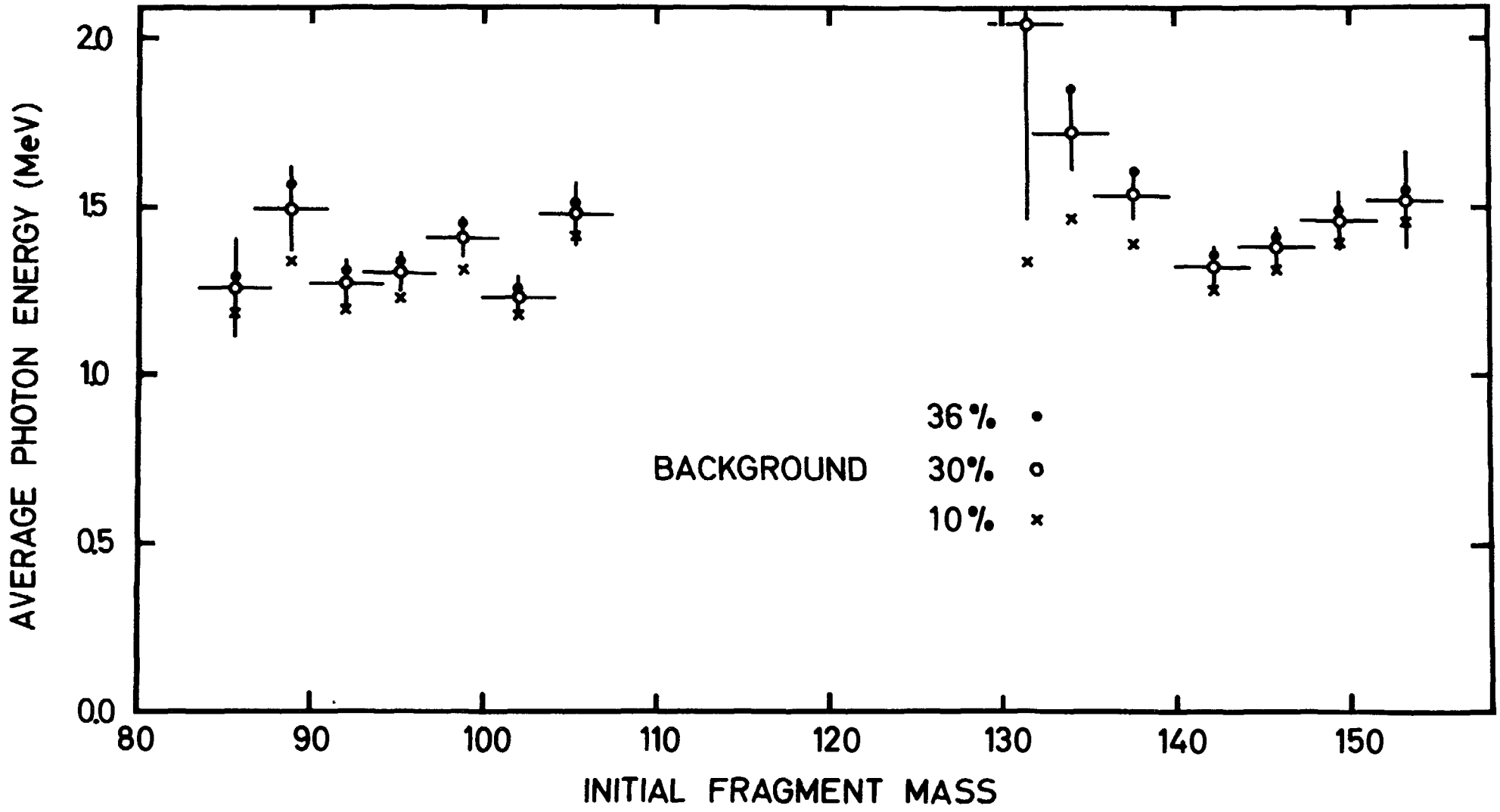

Fig. 7. The average energy per photon

LIST OF PUBLISHED AE-REPORTS

1–300. (See the back cover earlier reports.)

301. *The present status of the half-life measuring equipment and technique at* Studsvik. By S. G. Malmskog. 1967. 26 p. Sw. cr. 10:–.
302. Determination of oxygen in aluminum by means of 14 MeV neutrons with an account of flux attenuation in the sample. By D. Brune and K. Jirlow. 1967. 16 p. Sw. cr. 10:–.
303. Neutron elastic scattering cross sections of the elements Ni, Co, and Cu between 1.5 and 8.0 mev. By B. Holmqvist and T. Wiedling. 1967. 17 p. Sw. cr. 10:–.
304. A study of the energy dependence of the Th232 capture cross section in the energy region O.1 to 3.4 eV. By G. Lundgren. 1967. 25 p. Sw. cr. 10:–.
305. Studies of the reactivity effect of polythene in the fast reactor FRO. By L. I. Tirén and R. Håkansson. 1967. 25 p. Sw. cr. 10:–.
306. Final report on IFA-10, the first Swedish instrumented fuel assembly irradiated in HBWR, Norway. By J-A. Gyllander. 1967. 35 p. Sw. cr. 10:–.
307. Solution of large systems of linear equations with quadratic or non-quadratic matrices and deconvolution of spectra. By K. Nygaard. 1967. 15 p. Sw. cr. 10:–.
308. Irradiation of superheater test fuel elements in the steam loop of the R2 reactor. By F. Ravndal. 1967. 94 p. Sw. cr. 10:–.
309. Measurement of the decay of thermal neutrons in water poisoned with the non-1/v neutron absorber cadmium. By. L. G. Larsson and E. Möller. 1967. 20 p. Sw. cr. 10:–.
310. Calculated absolute detection efficiencies of cylindrical NaI (Tl) scintillation crystals for aqueous spherical sources. By. O. Strindehag and B. Tollander. 1968. 18 p. Sw. cr. 10:–.
311. Spectroscopic study of recombination in the early afterglow of a helium plasma. By J. Stevefelt. 1968. 49 p. Sw. cr. 10:–.
312. Report on the personnel dosimetry at AB Atomenergi during 1966. By J. Carlsson and T. Wahlberg. 1968. 10 p. Sw. cr. 10:–.
313. The electron temperature of a partially ionized gas in an electric field. By F. Robben. 1968. 16 p. Sw. cr. 10:–.
314. Activation Doppler measurements on U238 and U235 in some fast reactor spectra. By L. I. Tirén and I. Gustafsson. 1968. 40 p. Sw. cr. 10:–.
315. Transient temperature distribution in a reactor core with cylindrical fuel rods and compressible coolant. By H. Vollmer. 1968. 38 p. Sw. cr. 10:–.
316. Linear dynamics model for steam cooled fast power reactors. By H. Vollmer. 1968. 40 p. Sw. cr. 10:–.
317. A low level radioactivity monitor for aqueous waste. By E. J. M. Quirk. 1968. 35 p. Sw. cr. 10:–.
318. A study of the temperature distribution in UO_2 reactor fuel elements. By I. Devold. 1968. 82 p. Sw. cr. 10:–.
319. An on-line water monitor for low level β-radioactivity measurements. By E. J. M. Quirk. 1968. 26 p. Sw. cr. 10:–.
320. Special cryostats for lithium compensated germanium detectors. By A. Lauber, B. Malmsten and B. Rosencrantz. 1968. 14 p. Sw. cr. 10:–.
321. Stability of a steam cooled fast power reactor, its transients due to moderate perturbations and accidents. By H. Vollmer. 1968. 36 p. Sw. cr. 10:–.
322. Progress report 1967. Nuclear chemistry. 1968. 30 p. Sw. cr. 10:–.
323. Noise in the measurement of light with photomultipliers. By F. Robben. 1968. 74 p. Sw. cr. 10:–.
324. Theoretical investigation of an electrogasdynamic generator. By S. Palmgren. 1968. 36 p. Sw. cr. 10:–.
325. Some comparisons of measured and predicted primary radiation levels in the Ågesta power plant. By E. Aalto, R Sandlin and A. Krell. 1968. 44 p. Sw. cr. 10:–.
326. An investigation of an irradiated fuel pin by measurement of the production of fast neutrons in a thermal column and by pile oscillation technique. By Veine Gustavsson. 1968. 24 p. Sw. cr. 10:–.
327. Phytoplankton from Tvären, a bay of the Baltic, 1961–1963. By Torbjörn Willén. 1968. 76 p. Sw. 10:–.
328. Electronic contributions to the phonon damping in metals. By Rune Jonson. 1968. 38 p. Sw. cr. 10:–.
329. Calculation of resonance interaction effects using e rational approximation to the symmetric resonance line shape function. By H. Häggblom. 1968. 48 p. Sw. cr. 10:–.
330. Studies of the effect of heavy water in the fast reactor FRO. By L. I. Tirén, R. Håkansson and B. Karmhag. 1968. 26 p. Sw. cr. 10:–.
331. A comparison of theoretical and experimental values of the activation Doppler effect in some fast reactor spectra. By H. Häggblom and L. I. Tirén. 1968. 28 p. Sw. cr. 10:–.
332. Aspects of low temperature irradiation in neutron activation analysis. By D. Brune. 1968. 12 p. Sw. cr. 10:–.
333. Application of a betatron in photonuclear activation analysis. By D. Brune, S. Mattsson and K. Lidén. 1968. 13 p. Sw. cr. 10:–.
334. Computation of resonance-screened cross section by the Dorix-Speng system. By H. Häggblom. 1968. 34 p. Sw. cr. 10:–.
335. Solution of large systems of linear equations in the presence of errors. A constructive criticism of the least squares method. By K. Nygaard. 1968. 28 p. Sw. cr. 10:–.
336. Calculation of void volume fraction in the subcooled and quality boiling regions. By S. Z. Rouhani and E. Axelsson. 1968. 26 p. Sw. cr. 10:–.
337. Neutron elastic scattering cross sections of iron and zinc in the energy region 2.5 to 8.1 MeV. By B. Holmqvist, S. G. Johansson, A. Kiss, G. Lodin and T. Wiedling. 1968. 30 p. Sw. cr. 10:–.
338. Calibration experiments with a DISA hot-wire anemometer. By B. Kjellström and S. Hedberg. 1968. 112 p. Sw. cr. 10:–.
339. Silicon diode dosimeter for fast neutrons. By L. Svansson, P. Swedberg, C-O. Widell and M. Wik. 1968. 42 p. Sw. cr. 10:–.
340. Phase diagrams of some sodium and potassium salts in light and heavy water. By K. E. Holmberg. 1968 48 p. Sw. cr. 10:–.
341. Nonlinear dynamic model of power plants with single-phase coolant reactors. By H. Vollmer. 1968. 26 p. Sw. cr. 10:–.
342. Report on the personnel dosimetry at AB Atomenergi during 1967. By J. Carlsson and T. Wahlberg. 1968. 10 p. Sw. cr. 10:–.
343. Friction factors in rough rod bundles estimated from experiments in partially rough annuli – effects of dissimilarities in the shear stress and turbulence distributions. By B. Kjellström. 1968. 22 p. Sw. cr. 10:–.
344. A study of the resonance interaction effect between ^{238}U and ^{239}Pu in the lower energy region. By H. Häggblom. 1968. 48 p. Sw. cr. 10:–.
345. Application of the microwave discharge modification of the Wilzbach technique for the tritium labelling of some organics of biological interest. By T. Gosztonyi. 1968. 12 p. Sw. cr. 10:–.
346. A comparison between effective cross section calculations using the intermediate resonance approximation and more exact methods. By H. Häggblom. 1969. 64 p. Sw. cr. 10:–.
347. A parameter study of large fast reactor nuclear explosion accidents. By J. R. Wiesel. 1969. 34 p. Sw. cr. 10:–.
348. Computer program for inelastic neutron scattering by an anharmonic crystal. By L. Bohlin, I. Ebbsjö and T. Högberg. 1969. 52 p. Sw. cr. 10:–.
349. On low energy levels in ^{185}W. By S. G. Malmskog, M. Höjeberg and V. Berg. 1969. 18 p. Sw. cr. 10:–.
350. Formation of negative metal ions in a field-free plasma. By E. Larsson. 1969. 32 p. Sw. cr. 10:–.
351. A determination of the 2 200 m/s absorption cross section and resonance integral of arsenic by pile oscillator technique. By E. K. Sokolowski and R. Bladh. 1969. 14 p. Sw. cr. 10:–.
352. The decay of ^{191}Os. By S. G. Malmskog and A. Bäcklin. 1969. 24 p. Sw. cr. 10:–.
353. Diffusion from a ground level point source experiment with thermoluminescence dosimeters and Kr 85 as tracer substance. By Ch. Gyllander, S. Hollman and U. Widemo. 1969. 23 p. Sw. cr. 10:–.
354. Progress report, FFN, october 1, 1967 – september 30, 1968. By T. Wiedling. 1969. 35 p. Sw. cr. 10:–.
355. Thermodynamic analysis of a supercritical mercury power cycle. By A. S. Roberts, Jr., 1969. 25 p. Sw. cr. 10:–.
356. On the theory of compensation in lithium drifted semiconductor detectors. By A. Lauber. 1969. 45 p. Sw. cr. 10:–.
357. Half-life measurements of levels in ^{75}As. By M. Höjeberg and S. G. Malmskog. 1969. 14 p. Sw. cr. 10:–.
358. A non-linear digital computer model requiring short computation time for studies concerning the hydrodynamics of the BWR. By F. Reisch and G. Vayssier. 1969. 38 p. Sw. cr. 10: –.
359. Vanadium beta emission detectors for reactor in-core neutron monitoring. I. Ö. Andersson and B. Söderlund. 1969. 26 p. Sw. cr. 10:–.
360. Progress report 1968 nuclear chemistry. 1969. 38 p. Sw. cr. 10:–.
361. A half-life measurement of the 343.4 keV level in ^{175}Lu. By M. Höjeberg and S. G. Malmskog. 1969. 10 p. Sw. cr. 10:–.
362. The application of thermoluminescence dosimeters to studies of released activity distributions. By B-I. Rudén. 1969. 36 p. Sw. cr. 10:–.
363. Transition rates in ^{161}Dy. By V. Berg and S. G. Malmskog. 1969. 32 p. Sw. cr. 10:–.
364. Control rod reactivity measurements in the Ågesta reactor with the pulsed neutron method. By K. Björeus. 1969. 44 p. Sw. cr. 10:–.
365. On phonons in simple metals II. Calculated dispersion curves in aluminium. By R. Johnson and A. Westin. 1969. 124 p. Sw. cr. 10:–.
366. Neutron elastic scattering cross sections. Experimental data and optical model cross section calculations. A compilation of neutron data from the Studsvik neutron physics laboratory. By B. Holmqvist and T. Wiedling. 1969. 212 p. Sw. cr. 10:–.
367. Gamma radiation from fission fragments. Experimental apparatus – mass spectrum resolution. By J. Higbie. 1969. 50 p. Sw. cr. 10:–.
368. Scandinavian radiation chemistry meeting Studsvik and Stockholm, september 17–19, 1969. By H. Christensen. 1969. 34 p. Sw. cr. 10:–.
369. Report on the personnel dosimetry at AB Atomenergi during 1968. By J. Carlsson and T. Wahlberg. 1969. 10 p. Sw. cr 10:–.
370. Absolute transition rates in ^{189}Ir. By S. G. Malmskog and V. Berg. 1969. 16 p. Sw. cr. 10:–.
371. Transition probabilities in the 1/2+(631) Band in ^{235}U. By M. Höjeberg and S. G. Malmskog. 1969. 18 p. Sw. cr. 10:–.
372. E2 and M1 transition probabilities in odd mass Hg nuclei. By V. Berg, A. Bäcklin, B. Fogelberg and S. G. Malmskog. 1969. 19 p. Sw. cr. 10:–.
373. An experimental study of the accuracy of compensation in lithium drifted germanium detectors. By A. Lauber and B. Malmsten. 1969. 25 p. Sw. cr. 10:–.
374. Gamma radiation from fission fragments. By J. Higbie. 1969. 22 p. Sw. cr. 10:–.

List of published AES-reports (In Swedish)

1. Analysis be means of gamma spectrometry. By D. Brune. 1961. 10 p. Sw. cr. 6:–.
2. Irradiation changes and neutron atmosphere in reactor pressure vessels-some points of view. By M. Grounes. 1962. 33 p. Sw. cr. 6:–.
3. Study of the elongation limit in mild steel. By G. Östberg and R. Attermo. 1963. 17 p. Sw. cr. 6:–.
4. Technical purchasing in the reactor field. By Erik Jonson. 1963. 64 p. Sw. cr. 8:–.
5. Ågesta nuclear power station. Summary of technical data, descriptions, etc. for the reactor. By B. Lilliehöök. 1964. 336 p. Sw. cr. 15:–.
6. Atom Day 1965. Summary of lectures and discussions. By S. Sandström. 1966. 321 p. Sw. cr. 15:–.
7. Building materials containing radium considered from the radiation protection point of view. By Stig O. W. Bergström and Tor Wahlberg. 1967. 26 p. Sw. cr. 10:–.

Additional copies available from the library of AB Atomenergi, Fack, S-611 01 Nyköping, Sweden.

EOS-tryckerierna, Stockholm 1969